Toxicology 315 (2014) 38–48

Contents lists available at ScienceDirect

Toxicology

journal homepage: www.elsevier.com/locate/toxicol

The role of the glutamatergic NMDA receptor in nanosilver-evoked neurotoxicity in primary cultures of cerebellar granule cells

Elżbieta Ziemińska [a], Aleksandra Stafiej [a], Lidia Strużyńska [b,*]

[a] Laboratory of Pharmaconeurochemistry, Department of Neurochemistry, Mossakowski Medical Research Centre, Polish Academy of Sciences, Pawińskiego 5, 02-106 Warsaw, Poland
[b] Laboratory of Pathoneurochemistry, Department of Neurochemistry, Mossakowski Medical Research Centre, Polish Academy of Sciences, Pawińskiego 5, 02-106 Warsaw, Poland

ARTICLE INFO

Article history:
Received 23 September 2013
Received in revised form 8 November 2013
Accepted 20 November 2013
Available online 28 November 2013

Keywords:
Nanosilver
Nanotoxicity
Excitotoxicity
MK-801
Calcium homeostasis
Reactive oxygen species

ABSTRACT

Nanoparticles are known to enter the vertebrate brain, but little is known about their neurotoxicity. The aim of this study is to investigate mechanisms of the contribution of AgNPs to neuronal cell death using primary cultures of rat cerebellar granule cells (CGCs). We tested the role of glutamatergic N-methyl-D-aspartate receptors (NMDA) in AgNP-evoked neurotoxicity using MK-801, a noncompetitive inhibitor of NMDAR. We used commercially available 0.2% PVP-coated AgNPs <100 nm in a concentration range of 2.5–75 μg/ml sonicated with fetal calf serum. After a 10 min incubation period, a dose-dependent increase in the uptake of $^{45}Ca^{2+}$ into neurons was observed in the presence of 25–75 μg/mL AgNPs which was completely abolished by addition of MK-801. Using the fluorescent dye fluo3 AM we observed an increase in the intracellular calcium level by 87% compared to control. ROS production was found to increase by about 30% over control after a 30-min incubation with 75 μg/mL AgNPs. Further, we observed a significant decrease in the mitochondrial potential during a 30-min incubation with AgNPs. Administration of MK-801 was found to provide a protective effect. Our results show that excitotoxicity *via* activation of NMDA receptor, followed by calcium imbalance, destabilization of mitochondrial function and ROS production, indicate an important mechanism involved in neurotoxicity evoked by AgNPs in cultured neurons.

1. Introduction

Silver nanoparticles (AgNPs) are commonly used in life sciences applications and have become recently one of the most commonly used nanomaterials (Ahamed et al., 2010). Nanosilver is used in medical products such as antibacterial fluids, wound dressings, implants and catheters because of its antibacterial properties much more effective that those of the ionic form of silver (Chaloupka et al., 2010; Chen and Schluesener, 2008; Kubik et al., 2005).

A number of reports on the toxicity of nanoparticles to human cells and organs have been published (AshaRani et al., 2009; Cortese-Krott et al., 2009; Greulich et al., 2011). Nanoparticles may be delivered to the human body by inhalation, or by topical, oral or intravenous administration. Blood mediates the transport of nanoparticles mainly to the liver, lungs and spleen but they can also be found in kidney, brain, heart and testes (Lankveld et al., 2010; Loeschner et al., 2011). Nanoparticles, including nanosilver, may also reach the brain *via* the upper respiratory tract and sensory nerves in the olfactory bulb (Oberdörster et al., 2009) or by permeating the blood–brain barrier by endocytosis or passive diffusion (Hoet et al., 2004). The toxic effects of silver nanoparticles in the brain are of importance firstly due to observations of significant accumulation of silver in the brain relative to other organs (Rungby and Danscher, 1983) and secondly due to high susceptibility of the brain to oxidative stress which underlies many neurodegenerative diseases (Casetta et al., 2005).

The toxicity of nanoparticles depends on their size. Smaller nanoparticles have a higher surface to volume ratio and this provides the basis for some of the unusual properties of nanoparticles, including increased reactivity and particle-to-cell contact (due to a larger number of particles) so as enhanced toxicity (Christian et al., 2008). In the case of silver nanoparticles, it is also considered that their toxicity is additionally related to silver ions being released from the metallic form of silver. Silver nanoparticles produce disturbances in mitochondrial function including perturbation of cellular respiration because of decreased ATP levels and increased free radical production leading to cell death (Costa et al., 2010; Foldbjerg et al., 2009). Piao and co-workers (2011) demonstrated that silver nanoparticles decrease levels of glutathione and induce cell apoptosis. In general, recent studies using different

* Corresponding author at: Department of Neurochemistry, Mossakowski Medical Research Centre, Polish Academy of Sciences, 5 Pawińskiego Str., 02-106 Warsaw, Poland. Tel.: +48 22 668 54 23; fax: +48 22 668 54 23.
E-mail address: lidkas@imdik.pan.pl (L. Strużyńska).

0300-483X/$ – see front matter © 2013 Elsevier Ireland Ltd. All rights reserved.
http://dx.doi.org/10.1016/j.tox.2013.11.008

experimental models indicate that the main mechanism of cytotoxicity of AgNPs depends on induction of reactive oxygen species (ROS) leading to oxidative stress (Haase et al., 2012; Rahman et al., 2009; Struzynski et al., 2013).

Other investigations have focused on the molecular mechanisms underlying the neuronal toxicity of nanosilver in either *in vitro* or *in vivo* experiments (Haase et al., 2012; Liu et al., 2011). However, a linkage has not been established between excitotoxicity and the processes contributing to nanosilver neurotoxicity. As there are links between overactivation of glutamate receptors, production of reactive oxygen species and the induction of oxidative/nitrosative stress (Bonfoco et al., 1995), it is interesting to examine these interrelationships under conditions of exposure to AgNPs.

Excitotoxicity is the most important mechanism leading to degeneration of glutamatergic neurons as a result of overactivation of the N-methyl-D-aspartate (NMDA) class of glutamate receptors. Changes in intracellular calcium levels and deregulation of intracellular calcium signaling pathways are linked to excitoxicity and consequently lead to free radical production, mitochondrial dysfunction, and cell death (Panieri et al., 2013; Zhivotovsky and Orrenius, 2011).

It has been shown that neuronal-enriched cultures respond to nanosilver with an increase in intracellular calcium levels (Haase et al., 2012). Calcium can be obtained by cells from the extracellular space or *via* release of calcium from intracellular stores in the endoplasmic reticulum and mitochondria (Gunter and Pfeiffer, 1990; Kristian and Siesjo, 1996). The most important gates of calcium influx into the cell are the ionotropic glutamatergic receptors, and the NMDA receptors are particularly important in this regard (Kristian and Siesjo, 1996). It has also been demonstrated that silver ions induce an increase in intracellular zinc levels, and zinc released to the synaptic space may activate adequate units of NMDA receptors in a concentration-dependent manner (Cortese-Krott et al., 2009). However, there is no information suggesting the existence of a similar mechanism in the case of nanosilver.

Thus, the aim of the present study was to investigate the molecular mechanisms contributing to nanosilver-evoked neuronal cell death. We tested a hypothesis concerning the involvement of glutamatergic NMDA receptors in neurotoxicity of AgNPs and investigated the rate of $^{45}Ca^{2+}$ uptake and changes in intracellular calcium homeostasis, production of reactive oxygen species (ROS), mitochondrial membrane potential and cellular viability in the presence of AgNPs and after treatment with MK-801, an antagonist of the glutamatergic NMDA receptor.

2. Materials and methods

2.1. Materials

Fluo-3 AM, 6-carboxy-2′,7′-dichlorofluorescein diacetate (DCF) and rhodamine 123 (R123) were obtained from Molecular Probes (Eugene, OR, USA). $^{45}CaCl_2$ was obtained from Polatom Sp. z o.o., Otwock – Swierk, Poland. Other chemicals, including AgNPs, and cell culture materials were purchased from Sigma-Aldrich Chemical Co. (St. Louis, MO). All reagents used were of analytical grade.

2.2. Cell culture

Primary cultures of cerebellar granule cells (CGC) were prepared from 7-day-old male and female Wistar rats according to the method of Schousboe et al. (1985), with slight modifications as described previously (Zieminska et al., 2003, 2006, 2010).

The use of rat pups was in accordance with international standards of animal care guidelines. Procedures were approved by the Local Care of Experimental Animals Committee.

The rat pups were decapitated and the cerebella were rapidly removed. After separation of the vessels, the collected cerebella were cut into 400 μm cubes. Tissue was incubated for 15 min at 37 °C in ionic buffer containing 0.025% trypsin and 0.05% DNase 1. The incubation was terminated by addition of a type I soybean trypsin inhibitor (0.04%) and centrifugation. The cells were separated by trituration of the pellet with subsequent centrifugation. The cell suspension in basal Eagle's medium (BME) supplemented with 10% fetal calf serum, 25 mM KCl, 4 mM glutamine, streptomycin (50 μg/ml) and penicillin (50 U/ml) was used to seed 6-, 12- or 24-well plates (NUNC) coated with poly-L-lysine, at a density of 4, 2 or 1×10^6 cells per well. To prevent the replication of non-neuronal cells, cytosine arabinofuranoside was added to the cultures to a concentration of 7.5 μM 36 h after plating. The CGC were used in experiments after 7 days *in vitro*.

2.3. Preparation of silver nanoparticles

In the present study commercially-available AgNPs were used. The AgNPs were defined as a mixture of polyvinylpyrrolidone-coated nanoparticles (0.2% PVP-coated AgNPs) less than 100 nm in diameter as characterized by the manufacturer (http://www.sigmaaldrich.com/materials-science/nanomaterials/silver-nanoparticles.html). This material was previously investigated in toxicological studies (Park et al., 2010; Struzynski et al., 2013). Characterization of the degree of dispersion and particle size distribution was performed by transmission electron microscopy (JEM-1200EX, Jeol) according to a standard method. Before addition to the CGC culture (2×10^6/well), AgNPs were sonicated with fetal calf serum using a Bandelin SONOPLUS HD 70 sonicator (6 s × 20 s, 35W) to prevent sedimentation and agglomeration of nanoparticles. Terms of this procedure avoid heating of the solution and denaturation of serum proteins. Additionally AgNPs were filtered using 0.22 μM pore size filters. It has been demonstrated that the duration and power of sonication is significant (Cronholm et al., 2011), although a universal protocol for preparation of AgNPs prior to use has not yet been developed.

The same volume of supernatant (obtained after centrifugation at 15,000 × *g* for 30 min of the above-described AgNPs) containing Ag^+ liberated from AgNPs was used as a control. Stock solutions were freshly prepared before use in order to avoid sedimentation and agglomeration of nanoparticles and to reduce the release of Ag^+ ions from the metallic form of silver to the serum (Kittler et al., 2010). We check that nanoparticles were stable in solution during at least 48 h. Our analysis by mass spectroscopy (ICP MS Elan 6100 DRC Sciex Perkin Elmer, Canada) indicated that during that time concentration of liberated Ag^+ was very low and did not exceed much the amount measurable in fresh solution. We also observed that freezing of stock solutions of AgNPs up to −20 °C and thawing two weeks later, increases the Ag^+ concentration in the supernatant from 9.01 to 9.97 mg/L as compared to fresh solution. Alternatively, cold storage of a sample of a stock solution sample for two weeks at +4 °C was found to lead to significant release of Ag^+ ions from the initial concentration of 9.01 mg/L up to 15.27 mg/L.

2.4. Chronic AgNP-mediated neurotoxicity: induction and evaluation

On the 7th day of culture, a freshly prepared solution of AgNPs (according to above-described procedure) was added directly to BME growth medium to obtain final AgNPs concentrations in the range of 2.5–100 μg/mL. The concentration of AgNPs in the stock solution was calculated from the difference between the weight before and after filtration of 1 mL of serum containing nanoparticles. Supernatant containing Ag^+ liberated from the relevant concentration of nanoparticles prepared as described above was obtained after centrifugation at 15,000 × *g* for 30 min. Antagonist of glutamatergic NMDA receptor – 0.5 μM MK-801 – was used as a pharmacological tool. The effect of addition of antagonist was investigated.

The final culture medium contained AgNPs, supernatant (Ag^+) as a control, extra serum (as a control of the serum effect) or 0.5 μM MK-801, as required. The culture was maintained for 24 h. The cells were then fixed with 80% methanol, and stained with fluorescent dyes calcein and EtHD or with 0.5 μg/mL propidium iodide. Viable and dead neurons were counted using a fluorescence microscope (Zeiss-Axiovert, Germany) by a technician who was unaware of the details of the experiment, as described previously (Zieminska et al., 2006, 2010). The results are expressed as percentages of live cells with respect to total cells.

2.5. Measurement of radioactive calcium uptake

The CGC (4×10^6/well) were pre-incubated at 37 °C for 10 min in Locke 5 medium containing 154 mM NaCl, 5 mM KCl, 4 mM $NaHCO_3$, 2.3 mM $CaCl_2$, 5 mM HEPES (pH 7.4) and 5 mM glucose. Radioactive calcium (1 μCi/well) was then added together with 0.5 μM MK-801 and 2.5–100 μg/mL of AgNPs. After 10 min incubation at 37 °C the cells were washed three times with ice cold glucose and calcium-free medium containing 2 mM EGTA, lysed in 0.5 M NaOH. Radioactive uptake was measured using a Wallac 1409 liquid scintillation counter (Wallac, Turku, Finland).

2.6. Loading of cells with fluo-3 AM and fluorescence measurements

CGC (1×10^6/well) were loaded with 16 μM of the fluorescent calcium-sensitive probe fluo-3 AM, at 37 °C for 30 min in the original growth medium. The loading was terminated by washing the cells three times with Locke 5 buffer. The change in fluorescence after addition of each of the tested compounds was recorded at 1 min intervals over a 30 min. Incubation period, using a microplate reader (FLUOstar Omega, Germany) at 485 nm excitation and 538 nm emission wavelengths.

2.7. Measurement of mitochondrial membrane potential in CGC

Changes in mitochondrial membrane potential were monitored using rhodamine123 (R123). Depolarization of the membrane results in loss of R123 from the mitochondria and in increased intracellular fluorescence. R123 was added to cultures (1×10^6/well) to a final concentration of 10 μM for 30 min at 37 °C. The cells were then washed with Locke 5 buffer and treated with 75 μg/mL AgNPs or supernatant with or without MK-801 for 60 min. Changes in fluorescence were recorded at 3 min intervals, over a 1 h incubation period, using a microplate reader (Fluoroscan, LabScan, Finland) at 485 nm excitation and 538 nm emission wavelengths.

2.8. Measurement of free radical production in CGC

Changes in free radical production were evaluated using the fluorescent dye 2′,7′-dichlorofluorescein diacetate (DCF). DCF was added to cultures to a final concentration of 100 μM for 30 min at 37 °C. The cells (1×10^6/well) were then washed with Locke 5 buffer and treated with 75 μg/mL AgNPs or supernatant alone or together with MK-801 for 30 min. Changes in fluorescence were recorded at 1 min intervals over this period of incubation, using a microplate reader (FLUOstar Omega, Germany) at 485 nm excitation and 538 nm emission wavelengths.

2.9. Statistical analysis

Statistical analyses were performed using 3–5 of newly prepared cultures. Results are expressed as mean ± SD from the distinct experiments performed using the number of cultures indicated below each figure. Inter-group comparisons were made using the one-way analysis of variance (ANOVA). The significance level was set as $p < 0.05$.

3. Results

3.1. Silver nanoparticles

In our experiments we used commercially-available 0.2% polyvinylpyrrolidone (PVP)-coated AgNPs < 100 nm. Using TEM we observed that AgNPs were spherical and did not aggregate in stock solution in the presence of serum (Fig. 1B). The size distribution of nanoparticles was calculated from 15 electron micrographs of silver nanoparticles prepared by the procedure described in Section 2.3. The data are presented in a bar chart (Fig. 1A). More than 85% of AgNPs were between 5 and 25 nm. Less than 15% of nanoparticles did not exceed 35 nm. Supernatant obtained after centrifugation of the stock solution of AgNPs did not contain TEM-detectable nanoparticles.

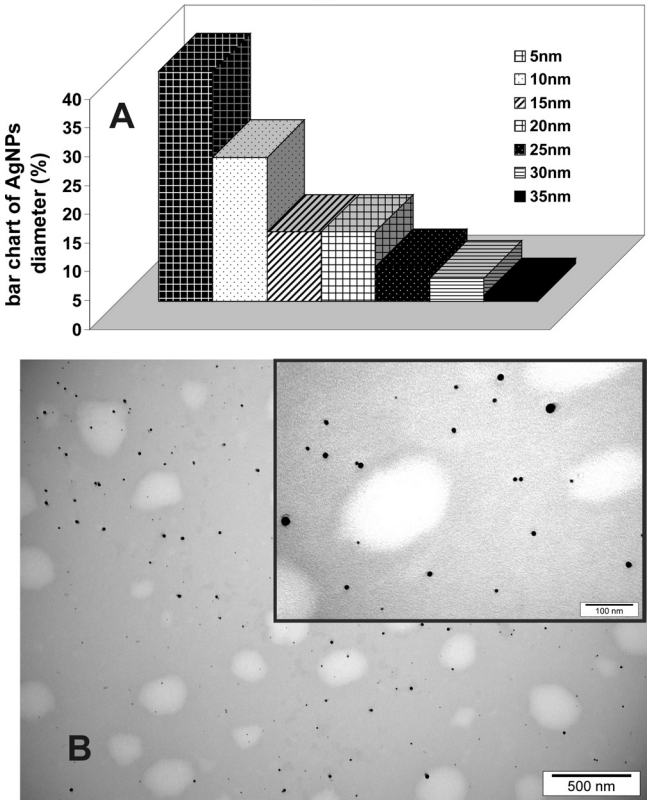

Fig. 1. A typical TEM image of AgNPs dispersed in serum (B) and the size distribution histogram (A) generated using 15 images captured by electron microscopy showing nanoparticles ranging in size between 5 and 35 nm. The analysis was performed using the stock solution after sonication and filtration.

3.2. Viability of CGC. The role of NMDA receptors

The number of live and dead neurons was assessed 24 h after addition of extra serum (Fig. 2A), supernatant (Ag^+) (Fig. 2B) or AgNPs (Fig. 2C). To visualize the cells, the fluorescent dyes calcein (green – live cells) and EtHD (red – dead neurons) (Fig. 2E) or propidium iodide (Fig. 2D) were used. More than 95% of control untreated cells exhibited green fluorescence indicating high viability (Fig. 2E). Addition of extra serum to the cultured neurons did not influence the viability of the cells in any case. Application of the same volume of supernatant (Ag^+) or AgNPs up to 25 μg/mL had no significant effect on the viability of neurons. The visible decrease in living cells with a parallel increase of dead cells occurred in a dose-dependent manner after addition of 50 μg/mL or greater doses of AgNPs. The results observed after addition of Ag^+ were generally comparable to an adequate dose of AgNPs but slightly greater numbers of cells survived.

In additional experiments, we used the concentration of nanoparticles in the presence of which viability of neurons decreased to about 50% of control (75 μg/mL). To determine the role of NMDA receptors in neurotoxicity of AgNPs, MK-801, a noncompetitive antagonist of NMDA receptors, was added. Incubation of cells in the presence of both AgNPs or Ag^+ together with this compound increased the viability of cells by about 30% or 25%, respectively (Fig. 2D).

3.3. Changes in $^{45}Ca^{+2}$ uptake and the intracellular calcium level in CG cells after incubation with AgNPs and an NMDAR antagonist

The 10-min exposure to nanoparticles in the concentration range of 25–75 μg/mL resulted in a dose-dependent increase in extracellular radioactive calcium uptake up to and exceeding the level obtained in the presence of 100 μM glutamate which was used as a positive control. This increase in calcium uptake was completely abolished by addition of 0.5 μM MK-801, a noncompetitive antagonist of NMDA receptors (Fig. 3A). Incubation with lower doses of AgNPs (2.5–10 μg/mL) did not exert the effect when compared to control cells cultured with serum (Fig. 3A). In the presence of supernatant-Ag^+ (50 μg/mL and 75 μg/mL) calcium uptake was found to be significantly lower than the calcium uptake observed for similar doses of AgNPs, although it increased significantly above the control value (Fig. 3B).

Since serum contains small amounts of its own glutamate, calcium and zinc ions (Ye and Sontheimer, 1998), it is necessary to compare the results obtained for AgNPs with control culture supplemented with the volume of serum (control + serum 25, 50 and 75 μg/mL) equal to the volume of AgNPs or supernatant-Ag^+ added to the experimental system (particularly when higher doses of AgNPs are used). Indeed, under these conditions, the uptake of Ca^{2+} was found to increase significantly above the level of the control in the case of the two highest concentrations (Fig. 3B) in a manner similar to that observed for the supernatant-Ag^+. It should be stressed that AgNP-evoked enhancement of Ca^{2+} uptake was much more

strongly expressed and significantly different from all of the applied control systems (control, control + serum, supernatant-Ag^+).

The intracellular calcium level was monitored using the fluorescent dye fluo3-AM. The concentration of intracellular calcium depends upon its uptake from the extracellular space and release from intracellular stores. Thus, we divided this type of experiment into two parts according to the observed rate of extracellular radioactive calcium uptake (see: Fig. 3A) *i.e.* low calcium uptake (the low concentrations of AgNPs 2.5–10 μg/mL) and high calcium uptake – (high concentration of AgNPs 25–75 μg/mL). It can be seen in Fig. 4A and B that the AgNP-evoked dose-dependent increase in intracellular calcium concentration is completely inhibited by MK-801 in the presence of low doses of AgNPs (Fig. 4A) or only partially (Fig. 4B) when high concentrations of AgNPs are present. Thus, we expect that in the second situation, the increased intracellular calcium level is the result of the two processes upon which it depends (the enhanced uptake of calcium and its release from intracellular stores). Inhibition by MK-801 indicates the participation of NMDA receptors in this process. However, the results shown in Fig. 4A and B are an oversimplification of the real situation because they do not take into account the side effects of serum composition and zinc concentrations. The significant contribution of serum to the observed changes in fluorescence is seen in Fig. 5A and B. The results show that the effect of serum supplementation should be taken into account while estimating changes in intracellular calcium level after treatment with AgNPs. Serum is the medium in which we

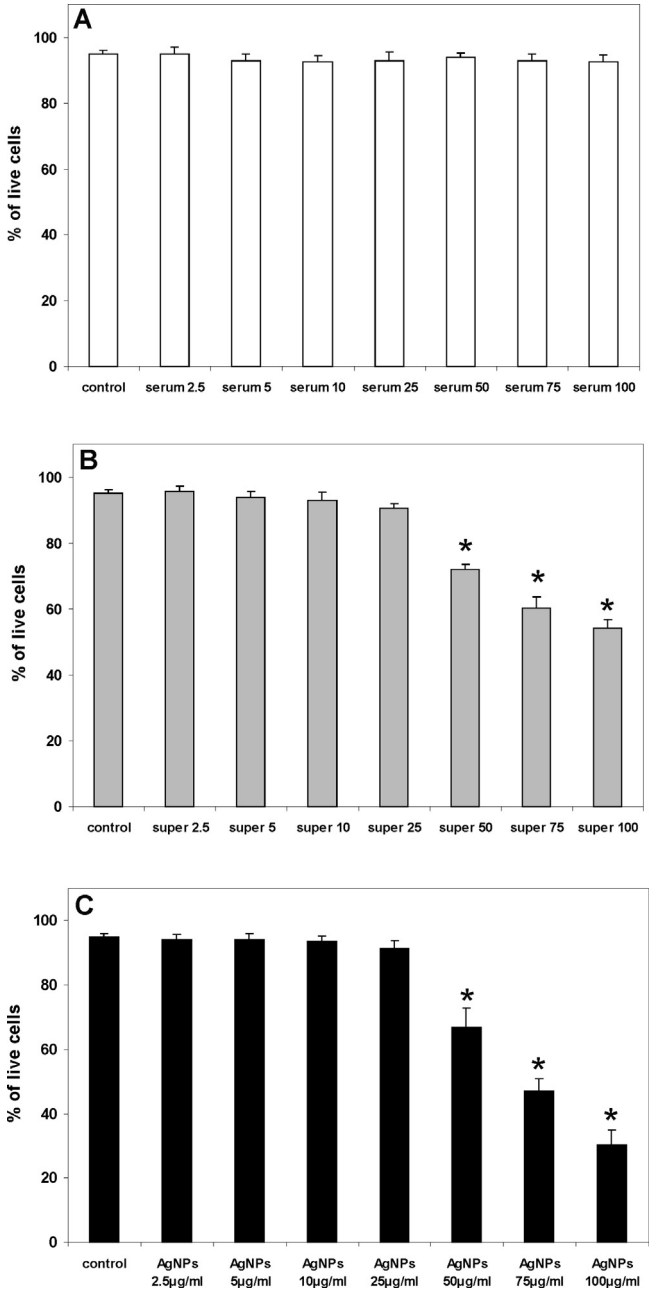

Fig. 2. The viability of CGC presented as a percentage of live cells: (A) in cultures supplemented with an additional amount of serum – control of the serum effect (B) in cultures treated with supernatant-Ag^+ – control of the effect of silver ions liberated from AgNPs and (C) exposed to AgNPs (2.5–100 μg/mL) presented as a dose effect. (D) The effect of MK-801. (E) Fluorescence image of control untreated cells and cells treated with 75 μg/mL of AgNPs; the living cells stained with calcein show green fluorescence, the dead cells stained with EtHD show red fluorescence. The results are presented as means ± SD from 4 independent experiments, $^*p < 0.05$ *vs.* control untreated cells; $^{\#}p < 0.05$ *vs.* culture without MK-801.

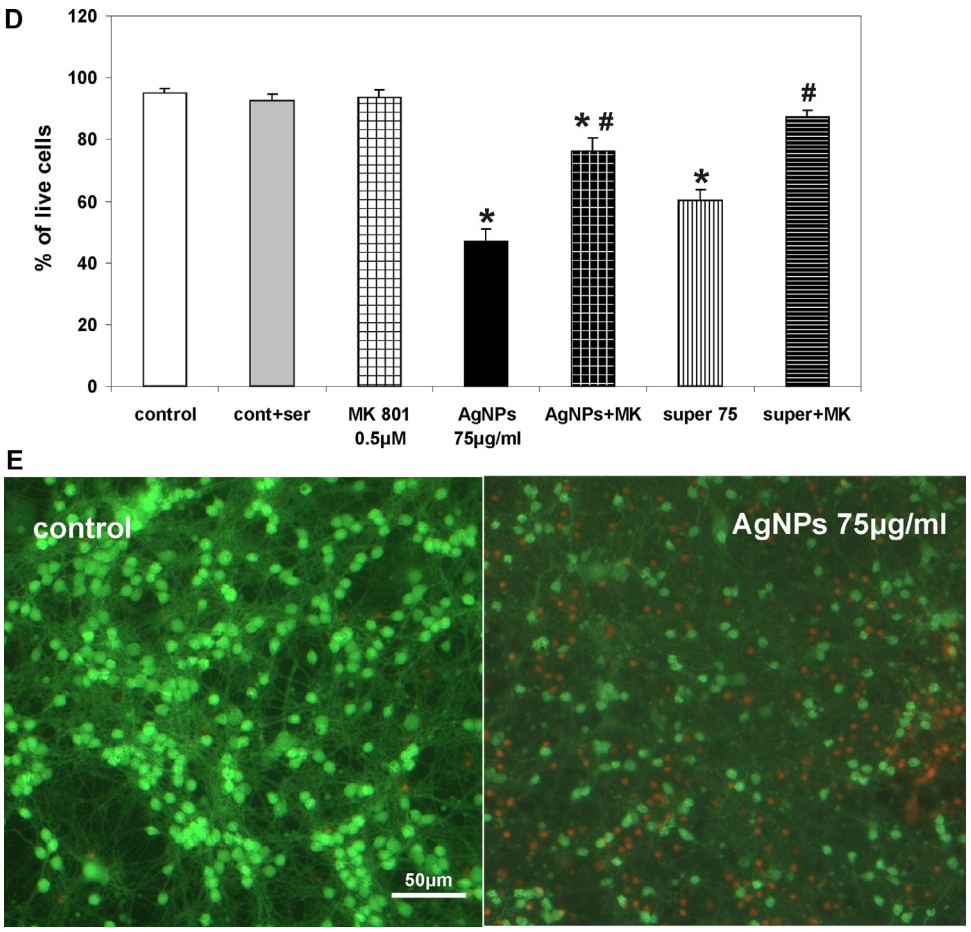

Fig. 2. (*Continued*)

"diluted" the silver nanoparticles. The presence of serum components such as glutamate, zinc or other divalent cations, affects the response of the cultured cells to intracellular calcium levels after addition either individually or together with nanoparticles. Thus, it is necessary to normalize the observations with respect to these factors. The results of our experiments are presented as the difference between the serum/nanoparticles response and the response of intact cells on fluo3 (control) in the time points. At each time point, the control exhibits value "0" on the *Y*-axis. It is can be seen that a significant increase in the level of fluorescence derived from serum occurs during the first minutes of measurement, (Fig. 5A and B). After the next few minutes, the fluorescence decreases and the response to the presence of AgNPs can be observed. With higher doses of AgNPs, the initial response to serum overlaps quickly with the proper response to the nanoparticles. In the presence of lower doses of AgNPs the maximal difference in fluorescence between serum 10 and control or AgNPs 10 and control was 15% in the 30th min of measurement. In the case of higher doses, the difference reached 40% (serum 75/control and AgNPs 75/control) in the 30th min of measurement. Differences in fluorescence measured in the 30th min for AgNPs and for adequate control (*i.e.* AgNPs 75-control and serum-control) are presented as Δ% in Fig. 5C. It can be seen that fluorescence increases dose-dependently for almost all of the concentrations in the range of 12–53% over control value.

Recent studies have revealed that virtually all fluorescent Ca^{2+} probes also bind Zn^{2+} ions. Therefore, changes in fluorescence of these probes often reflects the simultaneously occurring changes in the concentration of both ions, Ca^{2+} and Zn^{2+}, or sometimes of only Zn^{2+} ions (Dineley, 2007). In particular, Haase and coworkers (2009) demonstrated that the signal ascribed to Ca^{2+} in white blood cells, monitored with several fluorescent Ca^{2+} probes, was entirely due to Zn^{2+} ions. Therefore, we determined the extent to which the signals detected using fluo-3 are a result of zinc interference. In the experimental data presented in Fig. 6A and B we used TPEN [N,N,N,N-tetrakis(2-pyridylmethyl)ethylenediamine], a selective intracellular Zn^{2+} chelator, which is water-soluble and cell membrane permeable. Application of 20 μM TPEN to Locke 5 medium was found to slightly decrease the level of fluo-3 fluorescence. In this experiment we omitted the influence of serum alone to better demonstrate the proportion of Ca^{2+}:Zn^{2+} signal in the presence of different concentrations of AgNPs. After application of 2.5–10 μg/mL (Fig. 6A) and 25–75 μg/mL of AgNPs (Fig. 6B) fluorescence was found to increase in a dose-dependent manner. Administration of TPEN prior to addition of AgNPs in each case decreased the level of fluorescence evoked by AgNPs alone. The difference between the fluorescence value measured during the 30th min was found to be only a few percent for the low range of AgNPs whereas it increased significantly along with increasing concentrations of AgNPs (30–92% for 25–75 μg/mL of nanoparticles, respectively) (Fig. 6C). These results suggest that the total fluo-3 fluorescence signal depends on the dosage of AgNPs. This fluorescence is due to Ca^{2+} and Zn^{2+} signals in the proportion of 94%:6% while applying low doses. However, an enhanced contribution of Zn signal was observed in parallel increasing doses of AgNPs. The ratio was therefore changed and the proportion of Ca^{2+} to Zn^{2+} in the final signal was about 65%:35%.

As demonstrated above, the calcium response to the presence of nanoparticles is complex. Thus, we have included only representative results of various experiments for one dose of AgNPs to better

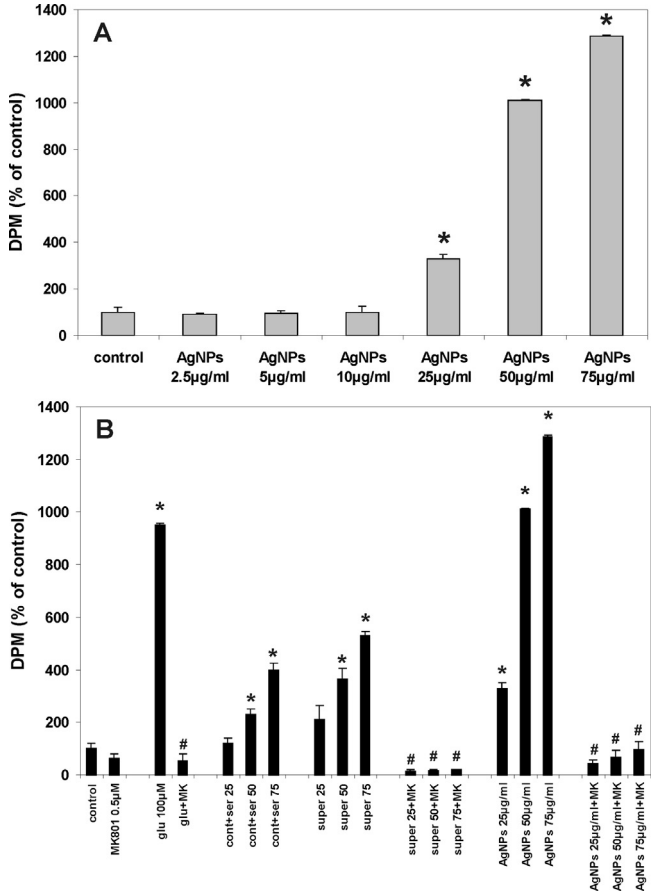

Fig. 3. Uptake of radioactive calcium by CGC exposed to different concentrations of AgNPs (A) and the effect of MK-801 (MK) a noncompetitive antagonist of NMDARs on calcium uptake in CGC exposed to AgNPs or supernatant-Ag^+ (B). Glutamate (glu), an agonist of NMDARs, was used as a positive control. Cultures of CGC supplemented with serum were used as a control of serum effect (control + ser). Accumulated $^{45}Ca^{2+}$ was measured in DPM and expressed as a percentage of untreated control. The results are presented as means ± SD from 4 independent experiments. $^*p < 0.05$ *vs.* control untreated cells. $^\#p < 0.05$ *vs.* culture without MK-801.

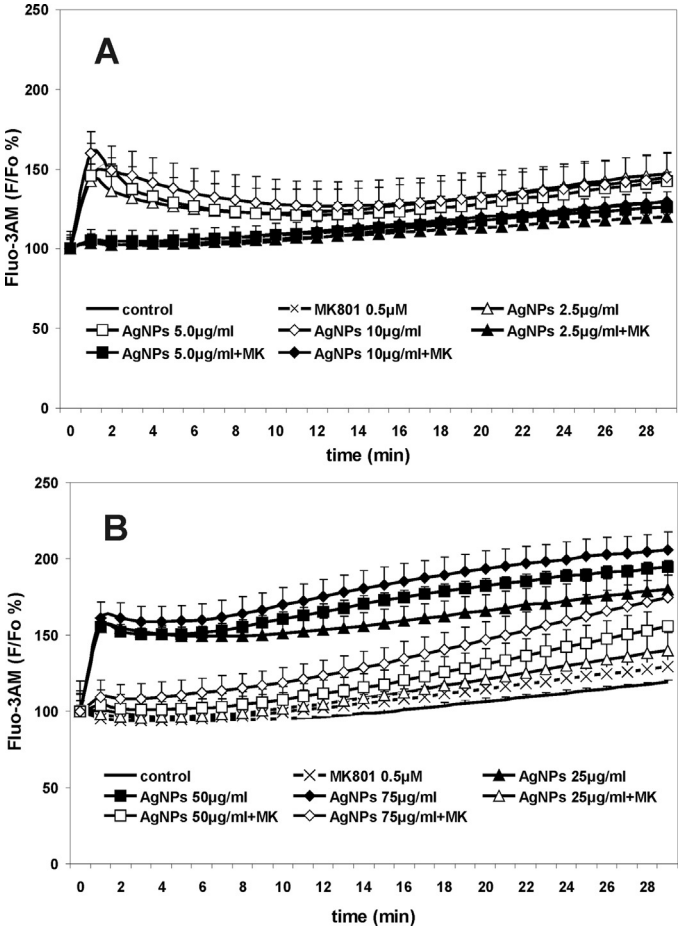

Fig. 4. The effect of MK-801, a noncompetitive antagonist of NMDARs, on the intracellular Ca^{2+} uptake into CGC cultured in the presence of low (A) and high (B) concentrations of AgNPs. Changes in the intracellular Ca^{2+} concentration measured as fluo-3 AM fluorescence were expressed relative to the basal level (fluo-3 AM F/Fo) as a percentage. The results are presented as means ± SD from 4 independent experiments.

illustrate the relationships between the same volume of AgNPs/Ag^+, calcium homeostasis and the role of the NMDA receptor in these mechanisms (Fig. 7). For the short-term experiment which employs Locke medium, we selected a concentration of 75 μg/mL to better visualize the responses of the intracellular calcium level, the mitochondrial membrane potential and production of ROS. When applying lower doses, a similar pattern of changes occurs to a lesser extent.

An increase in the intracellular calcium level after a 30-min incubation period of cells with 75 μg/mL AgNPs or Ag^+ reached 206% or 173%, respectively, relative to the initial level. This increase was significantly diminished by addition of 0.5 μM MK-801 in the presence of nanoparticles but not significantly in the presence of Ag^+ alone (by about 30% or 8%, respectively). These results indicate that disturbances in calcium homeostasis induced by exposure to AgNPs are mediated by the glutamatergic NMDA receptor.

3.4. Mitochondrial membrane potential and free radical production in CGC after addition of AgNPs and the NMDAR antagonist MK-801

In subsequent experiments, changes in the mitochondrial membrane potential in CGC were monitored using the fluorescent marker R123. Fig. 8 shows the effect of addition of 75 μg/mL AgNPs or Ag^+ alone or together with 0.5 μM MK-801 on R123 fluorescence. Both AgNPs and Ag^+ were found to induce a significant increase in the fluorescence by about 160% or 120% over the control, respectively. This reflects a drop in the mitochondrial membrane potential. MK-801 was found to decrease this effect in both cases by about 40%.

Production of ROS was measured using the fluorescent dye DCF. The fluorescence intensity of DCF increased by about 30% over control after a 30-min incubation with AgNPs and addition of MK-801 reduced the fluorescence intensity significantly (by about 20%). The increase in production of ROS evoked by Ag^+ (25% over control value) was only slightly reduced (by about 6%) by addition of MK-801 (Fig. 9).

4. Discussion

The objective of the present study was to assess the influence of silver nanoparticles on the viability of cultured rat cerebellar granule cells and to investigate the mechanisms leading to neuronal cell death with particular reference to the mechanism connected with overactivation of glutamatergic NMDA receptors. The results of our study confirmed the involvement of this receptor type in the neurotoxic effect evoked by PVP-coated silver nanoparticles in CGC.

The process of investigating nanoparticles in cultures encounters many methodological difficulties associated with their

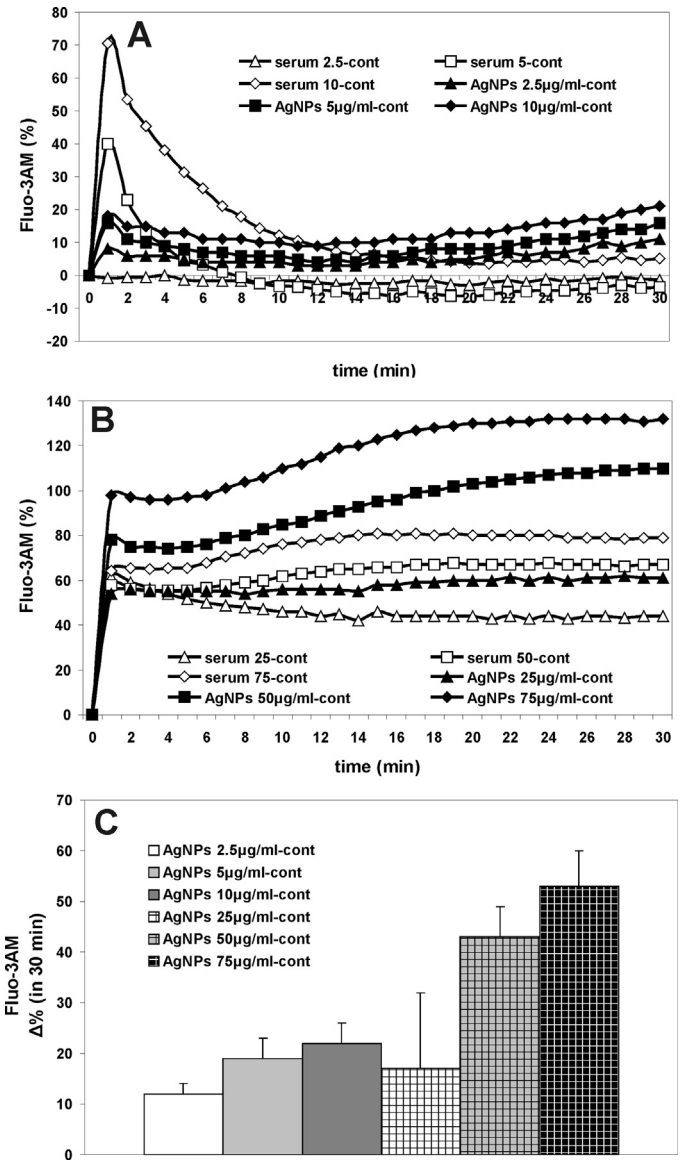

Fig. 5. The influence of extra serum supplementation on the intracellular calcium level in CGC cultured in the presence of low (A) or high (B) AgNPs concentrations. Differences in fluorescence measured during the 30th min between two points: AgNPs and corresponding control *i.e.* AgNPs 75-cont and serum-cont expressed as (Δ%) (C). The results are presented as means ± SD from 3 independent experiments.

addition to the growth medium. Nanoparticles have poor solubility in aqueous solutions and tend to agglomerate and sediment. Thus, prior to the addition to the cultures, nanoparticles should be evenly dispersed. Sonication in water did not result in a stable dispersed form. We therefore selected serum as a medium for sonication (Park et al., 2010). In serum, nanoparticles sediment very slowly and this characteristic provides reproducibility during addition to the cultures. However, in many cases, we observed, as a side-effect, an additional response of cells to this extra serum supplementation. Despite this observation, we elected to continue to use serum because it is expected to more closely replicate *in vivo* conditions where nanoparticles encounter blood serum proteins. Serum contains many additional components including, but not limited to albumins, glutamate, calcium, and zinc which can influence and alter the primary action of nanoparticles (Lesniak et al., 2010; Mariam et al., 2011; Ye and Sontheimer, 1998). Both Liu and colleagues (2009) and Gebregeorgis and co-workers (2013) showed that nanoparticles can bind to albumins and form new compounds. The sulfhydryl groups of albumin can assist in decreasing the toxicity evoked by metal ions such as Ag^{+} an Hg^{+2} (Divine et al., 1999; Zieminska et al., 2010).

It is known that silver nanoparticles can release silver ions and that these ions are partially responsible for the toxic action of nanoparticles on animal tissue or cell cultures. The effective participation of both forms of silver in the observed toxic effects has not yet been clarified (Beer et al., 2012; Lubick, 2008).

In our experiments we elected to use, as a control, supernatant obtained from a stock solution similar to the solution prepared for nanoparticles (see: Section 2), to recognize the component of the action resulting from nanoparticles and the component arising from silver ions. In this case we added an exact volume of serum containing silver ions or silver nanoparticles to the culture medium. Certainly this control does not accurately reflect the real situation but, from our point of view, it provides the closest possible conditions to biological conditions such as a cell culture. The concentration of ions remains stable during the entire experiment. In the case of nanoparticles, the concentration of the released silver ions tends to vary during the experiment because a fraction of AgNPs can be taken up by cells and the initial equilibrium between AgNPs and Ag^{+} can change, especially during the 24 h experiments conducted to investigate cellular viability. Although Ag nitrate or Ag acetate (Loeschner et al., 2011) are frequently used as controls, their greater toxicity necessitates the use of lower concentrations than the typical concentrations of nanoparticles.

In our opinion, there is no perfect control that reflects the real situation under experimental conditions as well *in vitro* as *in vivo* conditions in efforts to determine if nanoparticles or ions are responsible for toxicity and to determine the mechanisms of this toxicity.

The toxicity of nanoparticles depends on their type, size, coating, form, as well as on the type of culture/medium, concentration and duration of experiment (Carlson et al., 2008; Cronholm et al., 2013). The nanoparticles used in the present study are coated with nontoxic 0.2% PVP to prevent agglomeration of nanoparticles in powder. Dispersion of nanoparticles in serum stock solution was verified by transmission electron microscopy. As indicated in Fig. 1, we used nanoparticles ranging in size from 5 to 35 nm. However, 85% of the particles were in the range between 5 and 25 nm and are thus considered in the mid-range with respect to size and toxic potential (Carlson et al., 2008).

The response to the same concentration of a toxin depends also on the type of cell culture. Cell lines originating from brain tissue tend to be more resistant to toxicity than primary cell cultures. In our experiments we investigated cultures of cerebellar granule neurons culture to test mechanism of excitotoxicity, because these cells possess many functional NMDA receptors. The present experiments used two concentration ranges: 2.5–10 μg/mL AgNPs without observation of death of neurons, and 25–75 μg/mL when the viability of cells was observed to decrease in a dose-dependent manner to approximately 50% of the control.

Our results revealed that destabilization of calcium homeostasis is one of the main potential mechanisms of AgNPs neurotoxicity. We verified that exposure to AgNPs may intensify the entry of extracellular calcium into cultured neurons which further may lead to destabilization of the intracellular pool of calcium. The 10-min exposure to nanoparticles in concentrations between 25 and 75 μg/mL resulted in a dose-dependent increase in extracellular calcium uptake which exceeds the level evoked by 100 μM glutamate (an agonist of NMDARs which was used as a positive control). This uptake was completely abolished by addition of 0.5 μM MK-801, a noncompetitive inhibitor of NMDA receptors. This result indicates a significant role of this receptor type in calcium uptake stimulated by AgNPs. Incubation with lower doses of AgNPs was found to have no effect when compared to control with serum.

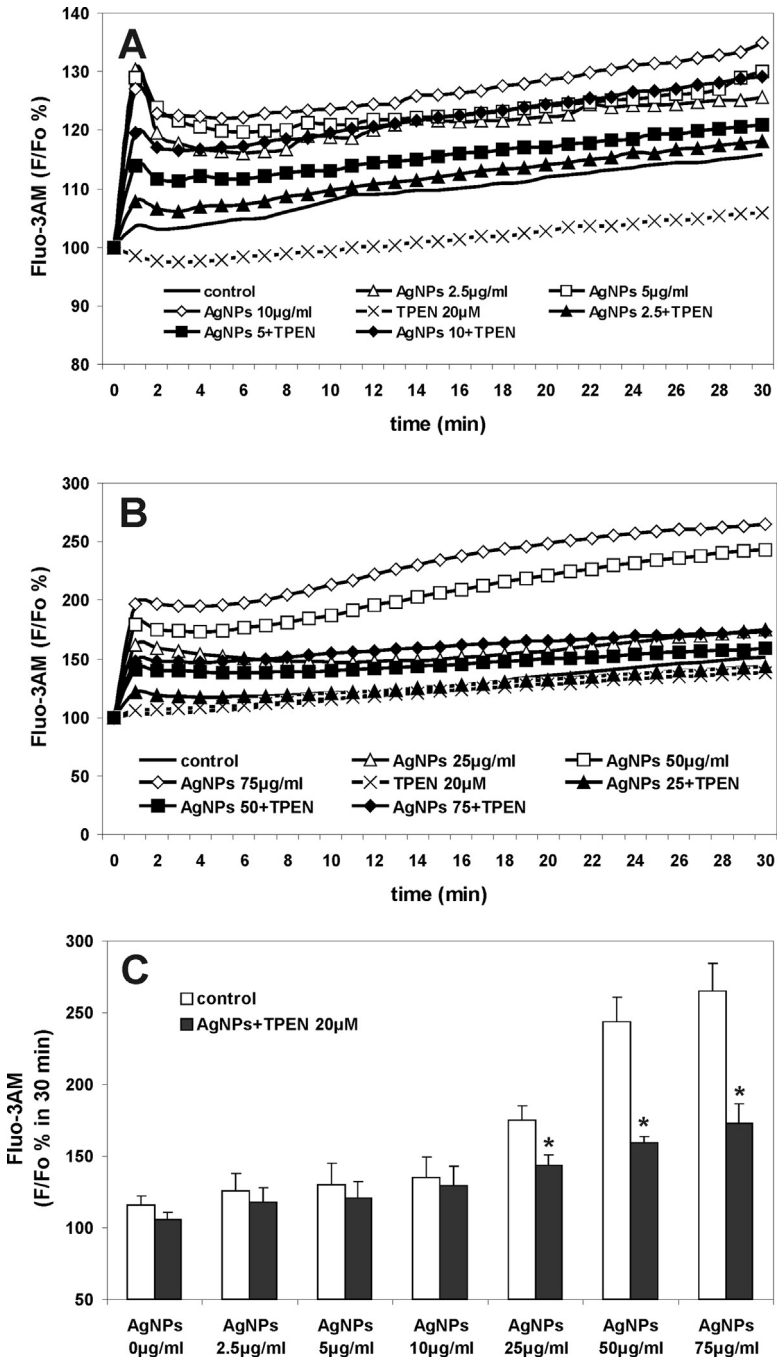

Fig. 6. The influence of zinc ions on the intracellular calcium level in CGC cultured in the presence of low (A) or high (B) AgNPs concentrations with or without TPEN which was used as a zinc chelator. Graph (C) indicates the contribution of the zinc signal in a whole fluo-3 fluorescence signal registered for CGC cultured with different doses of AgNPs. The results are presented as means ± SD from 3 independent experiments. $^{*}p < 0.05$ *vs.* control AgNPs-untreated cells.

In the presence of Ag^{+}, only a slight increase of radioactive calcium entry into the cells was observed relative to the increase observed for nanosilver. This indicates that the NMDAR-mediated phenomenon is mainly a characteristic response to nanosilver.

Similarly, AgNPs were found to evoke a dose-dependent increase in the intracellular calcium concentration. This observation is in agreement with previous results showing a strong and fast increase in the intracellular calcium level in neuronal-enriched cultures in response to addition of AgNPs (Haase et al., 2012). The antioxidant NAC applied by Haase and coworkers was found to have no effect on the calcium signals although it prevented the formation of ROS. The results of our study obtained after addition of MK-801 clearly indicate the involvement of NMDA receptors in disturbances of calcium homeostasis.

The key event caused by activation of the NMDA receptor is a massive influx of Ca^{2+} into neurons *via* the receptor's channel. This triggers the phenomenon of calcium-induced calcium release (CICR) from the endoplasmic reticulum stores (Lazarewicz et al., 1998).

With low doses of AgNPs, the increased intracellular calcium level was found to be completely inhibited by MK-801 while the rate of calcium uptake was not enhanced paralelly. A possible explanation is that the threshold of receptor activation is too low to elicit observable calcium uptake under the experimental

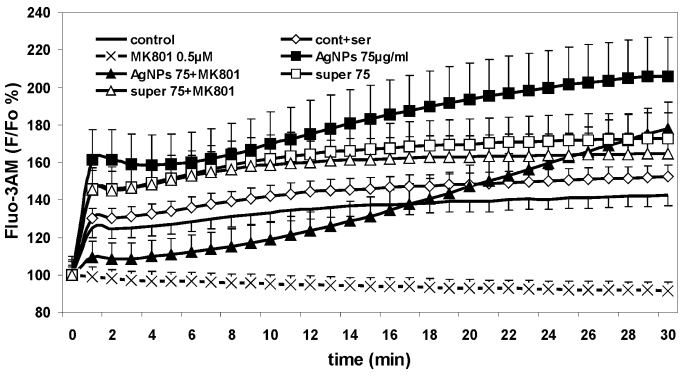

Fig. 7. The effect of MK-801, a noncompetitive antagonist of NMDARs, on the intracellular Ca^{2+} level in CGC cultured in the presence of 75 μg/mL AgNPs or supernatant-Ag^{+} (control of the effect of silver ions liberated from AgNPs in concentration of 75 μg/mL). Changes in the intracellular Ca^{2+} concentration measured as fluo-3 AM fluorescence were expressed relative to the basal level (fluo-3 AM F/Fo) as a percentage. The results are presented as means ± SD from 4 independent experiments.

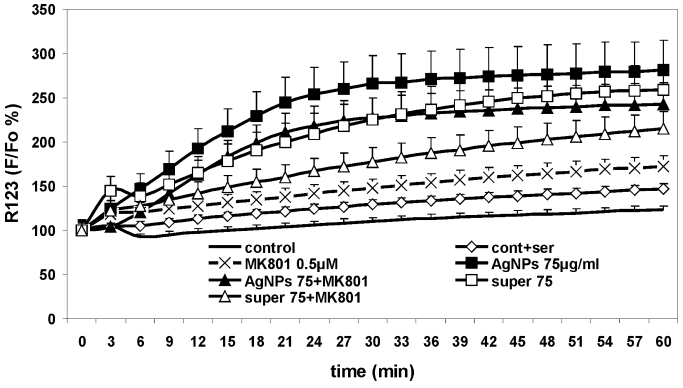

Fig. 8. Changes in the mitochondrial membrane potential in primary cultures of rat CGC exposed to 75 μg/mL of AgNPs or in the presence of MK-801, a noncompetitive antagonist of NMDRs. The basal fluorescence of cells loaded with rhodamine 123 (R123) was measured after 60 s. Increases in R123 fluorescence reflecting a reduction in the mitochondrial membrane potential are expressed relative to the basal level (R123 F/Fo) as a percentage. The results are means ± SD from five independent experiments.

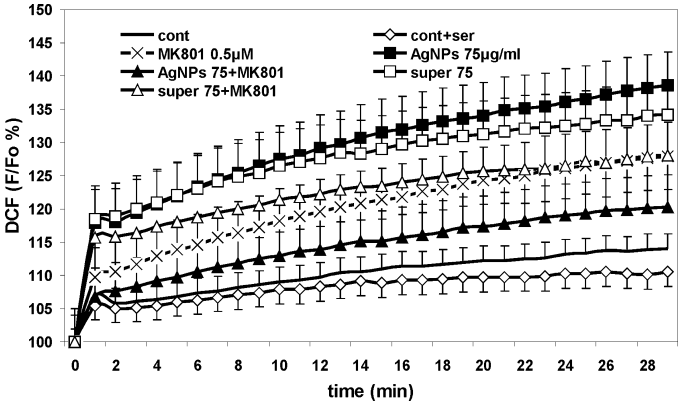

Fig. 9. Effect of MK-801, a noncompetitive antagonist of NMDRs, on the generation of reactive oxygen species (ROS) in CGC cultured in the presence of 75 μg/mL of AgNPs. ROS production was monitored using the fluorescent probe DCF. The basal DCF fluorescence of cells loaded with DCF was measured after 5 min. Increases in DCF fluorescence indicating enhanced ROS production are expressed relative to the basal level (DCF F/Fo) as a percentage. The results are means ± SD from five independent experiments.

conditions, although it is high enough to induce an increase in intracellular calcium by the mechanism of CICR. When high concentrations of AgNPs were added, an increase in the intracellular calcium level was observed and only partially reversed by addition of MK-801. This indicates that the increased calcium level is mediated by NMDARs and by a high rate of mobilization of calcium from intracellular stores. Experiments performed using TPEN have provided evidence of a significant contribution of Zn ions in this process. It is known that appropriate concentrations of Zn ions may activate (Paoletti et al., 2009) or directly inhibit (in higher concentrations > 20 μM) (Legendre and Westbrook, 1990; Paoletti et al., 1997) NMDA-sensitive glutamate-gated channels. It was also shown that intracellular Zn overload is correlated with neuronal death (Koh and Choi, 1994). Thus, it is possible that AgNPs themselves (or liberated Ag ions) may induce an increase in the intracellular zinc level and zinc can be further released to the synaptic space for activation of adequate units of NMDA receptors. A similar mechanism has been demonstrated for silver ions (Cortese-Krott et al., 2009). Alternatively, with AgNP exposure, an ionic imbalance among Ag^{+}, Zn^{2+} and Ca^{2+} is generated.

The results of our experiments which clarify the role of Zn in nanosilver-evoked CGC death will be presented in a separate report. However, it is evident that increased concentration of AgNPs is connected with enhanced contribution of Zn in the process of NMDARs activation.

Importantly, addition of MK-801 did not reverse the observed increase in the intracellular calcium level in the case of supernatant-Ag^{+}. This leads us to propose that different mechanisms are responsible for the toxic effect of different forms of silver. These data suggest that AgNPs may disturb calcium homeostasis and interfere with calcium signaling pathways in CGC cells.

It is known that disturbances in calcium homeostasis may lead to cell injury and death (Orrenius et al., 1992). Indeed, impaired survival has been observed in macrophages and lung epithelial cells treated with AgNPs (Soto et al., 2007). Furthermore, it has been demonstrated that the decreased viability of apoptotic CGC is coupled to oxidative stress (Rahman et al., 2009). However, in contrast to our study applying the same cellular model, the viability of CGC treated with AgNPs at a concentration 10 μg/mL was reduced to 11%. Presumably, this discrepancy is due to the methodological differences. Under our conditions, nanoparticles were added as a suspension in serum instead of being added directly. Serum proteins, in particular albumin, may influence the real concentration of nanoparticles by binding to them and forming a protein corona (Lesniak et al., 2010; Schäffler et al., 2013). This phenomenon is responsible for lowering the activity of nanoparticles and may exert a protective effect against their toxicity (Mortensen et al., 2013).

Prolonged or excessive stimulation of glutamatergic receptors is the basis of the excitotoxicity phenomenon. The generally accepted hypothesis is that the primary driver of the mechanism of neuronal damage is provided by the overloading of neurons with calcium originating from extracellular space (Olney, 1971) *via* NMDA receptors (ionotropic glutamate receptors) which are recognized as the most important gate for Ca^{2+} entry (Kristian and Siesjo, 1996). It is believed that mitochondrial dysfunction is tightly connected to the mechanism of excitotoxic damage of neurons (Ichas and Mazat, 1998). In the presence of AgNPs at a dose causing the death of half of the number of cultured neurons, we observed both a decrease in the mitochondrial potential and intracellular formation of ROS which was partially reversed by addition of MK-801. In the situation where NMDA receptors are over-activated and calcium floods into the cytosol, mitochondria take up calcium and this results in failure of oxidative phosphorylation, generation of ROS generation and leads to necrosis (Orrenius, 2007; Salinska et al., 2005). Increased generation of ROS under conditions of AgNP toxicity has been noted previously in various cell cultures (Carlson et al., 2008; Yin et al.,

2013). However, it should be stressed that it had not been connected to NMDARs. Our results unquestionably indicate that the, almost in part, observed production of ROS is a consequence of overactivation of this type of receptor.

5. Conclusions

The results of our study indicate that the neurotoxic effect evoked by silver nanoparticles is partially mediated by the glutamatergic NMDA receptor. To our knowledge, the effects of exposure to silver nanoparticles on NMDA receptor-mediated events at the neurochemical level have not yet been studied. In CGC cultured in the presence AgNPs, we observed increased calcium uptake, intracellular calcium imbalance followed by decrease of mitochondrial membrane potential and enhanced ROS production with subsequent cell death. Most of these abnormalities were reversed fully or partially by addition of MK-801, a noncompetitive antagonist of the NMDA receptor. This indicates an important role of the excitotoxicity-like mechanism which is connected with overactivation of NMDARs but on the other hand indicates the possibility of other mechanisms contributing to nanosilver neurotoxicity.

Acknowledgments

This study was supported by funds from Polish Ministry of Science and Higher Education, [grant number NN 401619938].

We thank Dr. Małgorzata Frontczak-Baniewicz for her valuable contribution to the TEM studies.

References

Ahamed, M., Alsalhi, M.S., Siddiqui, M.K.J., 2010. Silver nanoparticle applications and human health. Clin. Chim. Acta 411, 1841–1848.

AshaRani, P.V., Mun, G.L.K., Hande, M.P., Valiyaveettil, S., 2009. Cytotoxicity and genotoxicity of silver nanoparticles in human cells. ACS Nano 3, 279–290.

Beer, C., Foldbjerg, R., Hayashi, Y., Sutherland, D.S., Autrup, H., 2012. Toxicity of silver nanoparticles – nanoparticle or silver ion? Toxicol. Lett. 208, 286–292.

Bonfoco, E., Krainc, D., Ankarcrona, M., Nicotera, P., Lepton, S.A., 1995. Apoptosis and necrosis: two distinct events induced, respectively, by mild and intense insults with N-methyl-D-aspartate or nitric oxide/superoxide in cortical cell cultures. Proc. Natl. Acad. Sci. U. S. A. 92, 7162–7166.

Carlson, C., Hussain, S.M., Schrand, A.M., Braydich-Stolle, L.K., Hess, K.L., Jones, R.L., Schlager, J.J., 2008. Unique cellular interaction of silver nanoparticles: size-dependent generation of reactive oxygen species. J. Phys. Chem. B 112, 13608–13619.

Casetta, I., Govoni, V., Granieri, E., 2005. Oxidative stress, antioxidants and neurodegenerative diseases. Curr. Pharm. Des. 11, 2033–2052.

Chaloupka, K., Malam, Y., Seifalian, A.M., 2010. Nanosilver as a new generation of nanoproduct in biomedical applications. Trends Biotechnol. 28, 580–588.

Chen, X., Schluesener, H.J., 2008. Nanosilver: a nanoproduct in medical application. Toxicol. Lett. 176, 1–12.

Christian, P., Von der Kammer, F., Baalousha, M., Hofmann, Th., 2008. Nanoparticles: structure, properties preparation and behaviour in environmental media. Ecotoxicology 17, 326–343.

Cortese-Krott, M.M., Münchow, M., Pirev, E., Hessner, F., Bozkurt, A., Uciechowski, P., Pallua, N., Kröncke, K.D., Suschek, C.V., 2009. Silver ions induce oxidative stress and intracellular zinc release in human skin fibroblasts. Free Radic. Biol. Med. 47, 1570–2157.

Costa, C.S., Ronconi, J.V., Daufenbach, J.F., Gonçalves, C.L., Rezin, G.T., Streck, E.L., Paula, M.M., 2010. In vitro effects of silver nanoparticles on the mitochondrial respiratory chain. Mol. Cell. Biochem. 342, 51–56.

Cronholm, P., Midander, K., Karlsson, H.L., Elihn, K., Wallinder, I.O., Möller, L., 2011. Effect of sonication and serum proteins on copper release from copper nanoparticles and the toxicity towards lung epithelial cells. Nanotoxicology 5, 269–281.

Cronholm, P., Karlsson, H.L., Hedberg, J., Lowe, T.A., Winnberg, L., Elihn, K., Wallinder, I.O., Möller, L., 2013. Intracellular uptake and toxicity of Ag and CuO nanoparticles: a comparison between nanoparticles and their corresponding metal ions. Small 9, 970–982.

Dineley, K.E., 2007. On the use of fluorescent probes to distinguish Ca2+ from Zn2+ in models of excitotoxicity. Cell Calcium 42, 341–342.

Divine, K.K., Ayala-Fierro, F., Barber, D.S., Carter, D.E., 1999. Glutathione, albumin, cysteine, and cys-gly effects on toxicity and accumulation of mercuric chloridein LLC-PK1 cells. J. Toxicol. Environ. Health A 57, 489–505.

Foldbjerg, R., Olesen, P., Hougaard, M., Dang, D.A., Hoffmann, H.J., Autrup, H., 2009. PVP-coated silver nanoparticles and silver ions induce reactive oxygen species, apoptosis and necrosis in THP-1 monocytes. Toxicol. Lett. 190, 156–162.

Gebregeorgis, A., Bhan, C., Wilson, O., Raghavan, D., 2013. Characterization of silver/bovine serum albumin (Ag/BSA) nanoparticles structure: morphological, compositional, and interaction studies. J. Colloid. Interface Sci. 389, 31–41.

Greulich, C., Diendorf, J., Simon, T., Eggeler, G., Epple, M., Köller, M., 2011. Uptake and intracellular distribution of silver nanoparticles in human mesenchymal stem cells. Acta Biomater. 7, 347–354.

Gunter, T.E., Pfeiffer, D.R., 1990. Mechanisms by which mitochondria transport calcium. Am. J. Physiol. 258, C755–C786.

Haase, H., Hebel, S., Engelhardt, G., Rink, L., 2009. Zinc ions cause the thimerosal induced signal of fluorescent calcium probes in lymphocytes. Cell Calcium 45, 185–191.

Haase, A., Rott, S., Mantion, A., Graf, P., Plendl, J., Thünemann, A.F., Meier, W.P., Taubert, A., Luch, A., Reiser, G., 2012. Effects of silver nanoparticles on primary mixed neural cell cultures: uptake, oxidative stress and acute calcium responses. Toxicol. Sci. 126, 457–468.

Hoet, P.H., Brüske-Hohlfeld, I., Salata, O.V., 2004. Nanoparticles – known and unknown health risks. J. Nanobiotechnol. 2, 12.

Ichas, F., Mazat, J.P., 1998. From calcium signaling to cell death: two conformations for the mitochondrial permeability transition pore, switching from low- to high-conductance state. Biochim. Biophys. Acta 1366, 33–50.

Kittler, S., Greulich, C., Diendorf, J., Köller, M., Epple, M., 2010. Toxicity of silver nanoparticles increases during storage because of slow dissolution under release of silver ions. Chem. Mater. 22, 4548–4554.

Koh, J.Y., Choi, D.W., 1994. Zinc toxicity on cultured cortical neurons: involvement of N-methyl-D-aspartate receptors. Neuroscience 60, 1049–1057.

Kristian, T., Siesjo, B.K., 1996. Calcium-related damage in ischemia. Life Sci. 59, 357–367.

Kubik, T., Bogunia-Kubik, K., Sugisaka, M., 2005. Nanotechnology on duty in medical applications. Curr. Pharm. Biotechnol. 6, 17–33.

Lankveld, D.P., Oomen, A.G., Krystek, P., Neigh, A., Troost-de Jong, A., Noorlander, C.W., Van Eijkeren, J.C., Geertsma, R.E., De Jong, W.H., 2010. The kinetics of the tissue distribution of silver nanoparticles of different sizes. Biomaterials 31, 8350–8361.

Lazarewicz, J.W., Rybkowski, W., Sadowski, M., Ziembowicz, A., Alaraj, M., Wegiel, J., Wisniewski, H.M., 1998. N-methyl-D-aspartate receptor-mediated, calcium-induced calcium release in rat dentate gyrus/CA4 in vivo. J. Neurosci. Res. 51, 76–84.

Legendre, P., Westbrook, G.L., 1990. The inhibition of single N-methyl-D-aspartate-activated channels by zinc ions on cultured rat neurons. J. Physiol. 429, 429–449.

Lesniak, A., Campbell, A., Monopoli, M.P., Lynch, I., Salvati, A., Dawson, K.A., 2010. Serum heat inactivation affects protein corona composition and nanoparticle uptake. Biomaterials 31, 9511–9518.

Liu, R., Sun, F., Zhang, L., Zong, W., Zhao, X., Wang, L., Wu, R., Hao, X., 2009. Evaluation on the toxicity of nanoAg to bovine serum albumin. Sci. Total. Environ. 407, 4184–4188.

Liu, Z., Ren, G., Zhang, T., Yang, Z., 2011. The inhibitory effects of nano-Ag on voltage-gated potassium currents of hippocampal CA1 neurons. Environ. Toxicol. 26, 552–558.

Loeschner, K., Hadrup, N., Qvortrup, K., Larsen, A., Gao, X., Vogel, U., Mortensen, A., Lam, H.R., Larsen, E.H., 2011. Distribution of silver in rats following 28 days of repeated oral exposure to silver nanoparticles or silver acetate. Part Fibre Toxicol. 8, 18.

Lubick, N., 2008. Nanosilver toxicity: ions, nanoparticles or both? Environ. Sci. Technol. 42, 8617–8620.

Mariam, J., Dongre, P.M., Kothari, D.C., 2011. Study of interaction of silver nanoparticles with bovine serum albumin using fluorescence spectroscopy. J. Fluoresc. 21, 2193–2199.

Mortensen, N.P., Hurst, G.B., Wang, W., Foster, C.M., Nallathamby, P.D., Retterer, S.T., 2013. Dynamic development of the protein corona on silica nanoparticles: composition and role in toxicity. Nanoscale 5, 6372–6380.

Oberdörster, G., Elder, A., Rinderknecht, A., 2009. Nanoparticles and the brain: couse of concern? J. Nanosci. Nanotechnol. 9, 4996–5007.

Olney, J.W., 1971. Glutamate-induced neuronal necrosis in the infant mouse hypothalamus. An electron microscopic study. J. Neuropathol. Exp. Neurol. 30, 75–90.

Orrenius, S., 2007. Reactive oxygen species in mitochondria-mediated cell death. Drug Metab. Rev. 39, 443–455.

Orrenius, S., McCabe Jr., M.J., Nicotera, P., 1992. Ca(2+)-dependent mechanisms of cytotoxicity and programmed cell death. Toxicol. Lett. 64/65, 357–364.

Panieri, E., Gogvadze, V., Norberg, E., Venkatesh, R., Orrenius, S., Zhivotovsky, B., 2013. Reactive oxygen species generated in different compartments induce cell death, survival, or senescence. Free Radic. Biol. Med. 57, 176–187.

Paoletti, P., Ascher, P., Neyton, J., 1997. High-affinity zinc inhibition of NMDA NR1-NR2A receptors. J. Neurosci. 17, 5711–5725.

Paoletti, P., Vergnano, A.M., Barbour, B., Casado, M., 2009. Zinc at glutamatergic synapses. Neuroscience 158, 126–136.

Park, E.J., Yi, J., Kim, Y., Choi, K., Park, K., 2010. Silver nanoparticles induce cytotoxicity by a Trojan-horse type mechanism. Toxicol. In Vitro 24, 872–878.

Piao, M.J., Kang, K.A., Lee, I.K., Kim, H.S., Kim, S., Choi, J.Y., Choi, J., Hyun, J.W., 2011. Silver nanoparticles induce oxidative cell damage in human liver cells through inhibition of reduced glutathione and induction of mitochondria-involved apoptosis. Toxicol. Lett. 201, 92–100.

Rahman, M.F., Wang, J., Patterson, T.A., Saini, U.T., Robinson, B.L., Newport, G.D., Murdock, R.C., Schlager, J.J., Hussain, S.M., Ali, S.F., 2009. Expression of genes related

to oxidative stress in the mouse brain after exposure to silver-25 nanoparticles. Toxicol. Lett. 197, 15–21.
Rungby, J., Danscher, G., 1983. Localization of exogenous silver in brain and spinal cord of silver exposed rats. Acta Neuropathol. 60, 92–98.
Salinska, E., Danysz, W., Lazarewicz, J.W., 2005. The role of excitotoxicity in neurodegeneration. Folia Neuropathol. 43, 322–339.
Schäffler, M., Semmler-Behnke, M., Sarioglu, H., Takenaka, S., Wenk, A., Schleh, C., Hauck, S.M., Johnston, B.D., Kreyling, W.G., 2013. Serum protein identification and quantification of the corona of 5, 15 and 80 nm gold nanoparticles. Nanotechnology 24, 265103.
Schousboe, A., Drejer, J., Hansen, G.H., Meier, E., 1985. Cultured neurons as model systems for biochemical and pharmacological studies on receptors for neurotransmitter amino acids. Dev. Neurosci. 7, 252–262.
Soto, K., Garza, K.M., Murr, L.E., 2007. Cytotoxic effects of aggregated nanomaterials. Acta Biomater. 3, 351–358.
Struzynski, W., Dabrowska-Bouta, B., Grygorowicz, T., Zieminska, E., Struzynska, L., 2013. Markers of oxidative stress in hepatopancreas of crayfish (orconectes limosus, raf) experimentally exposed to nanosilver. Environ. Toxicol., http://dx.doi.org/10.1002/tox.21859.
Ye, Z.C., Sontheimer, H., 1998. Astrocytes protect neurons from neurotoxic injury by serum glutamate. Glia 22, 237–248.
Yin, N., Liu, Q., Liu, J., He, B., Cui, L., Li, Z., Yun, Z., Qu, G., Liu, S., Zhou, Q., Jiang, G., 2013. Silver nanoparticle exposure attenuates the viability of rat cerebellum granule cells through apoptosis coupled to oxidative stress. Small 9, 1831–1841.
Zhivotovsky, B., Orrenius, S., 2011. Calcium and cell death mechanisms: a perspective from the cell death community. Cell Calcium 50, 211–221.
Zieminska, E., Stafiej, A., Lazarewicz, J.W., 2003. Role of group I metabotropic glutamate receptors and NMDA receptors in homocysteine-evoked acute neurodegeneration of cultured cerebellar granule neurones. Neurochem. Int. 43, 481–492.
Zieminska, E., Matyja, E., Kozlowska, H., Stafiej, A., Lazarewicz, J.W., 2006. Excitotoxic neuronal injury in acute homocysteine neurotoxicity: role of calcium and mitochondrial alterations. Neurochem. Int. 48, 491–497.
Zieminska, E., Toczylowska, B., Stafiej, A., Lazarewicz, J.W., 2010. Low molecular weight thiols reduce thimerosal neurotoxicity in vitro: modulation by proteins. Toxicology 276, 154–163.